

Planning and Rendering: Towards End-to-End Product Poster Generation

Zhaochen Li^{1,2*}, Fengheng Li^{1,3*}, Wei Feng^{1*}, Honghe Zhu¹, An Liu¹, Yaoyu Li¹, Zheng Zhang¹, Jingjing Lv¹, Xin Zhu¹, Junjie Shen¹, Zhangang Lin¹, Jingping Shao¹, Zhenglu Yang³
¹JD Retail Platform Operation and Marketing Center ²Peking University ³Nankai University
zhaochenli@pku.edu.cn, lifengheng@mail.nankai.edu.cn, {fengwei25, zhuhonghe1, liuan39, liyaoyu1, zhangzheng11, lvjingjing1, zhuxin3, shenjunjie, linzhangang, shaojingping}@jd.com, yangzl@nankai.edu.cn

Abstract

End-to-end product poster generation significantly optimizes design efficiency and reduces production costs. Prevailing methods predominantly rely on image-inpainting methods to generate clean background images for given products. Subsequently, poster layout generation methods are employed to produce corresponding layout results. However, the background images may not be suitable for accommodating textual content due to their complexity, and the fixed location of products limits the diversity of layout results. To alleviate these issues, we propose a novel product poster generation framework named P&R. The P&R draws inspiration from the workflow of designers in creating posters, which consists of two stages: Planning and Rendering. At the planning stage, we propose a PlanNet to generate the layout of the product and other visual components considering both the appearance features of the product and semantic features of the text, which improves the diversity and rationality of the layouts. At the rendering stage, we propose a RenderNet to generate the background for the product while considering the generated layout, where a spatial fusion module is introduced to fuse the layout of different visual components. To foster the advancement of this field, we propose the first end-to-end product poster generation dataset PPG30k, comprising 30k exquisite product poster images along with comprehensive image and text annotations. Our method outperforms the state-of-the-art product poster generation methods on PPG30k. The PPG30k will be released soon.

1. Introduction

Product posters are important for product promotion. An exquisite poster should not only have a rational layout of

* Authors contributed equally to this research

† Work done during an internship at JD.com

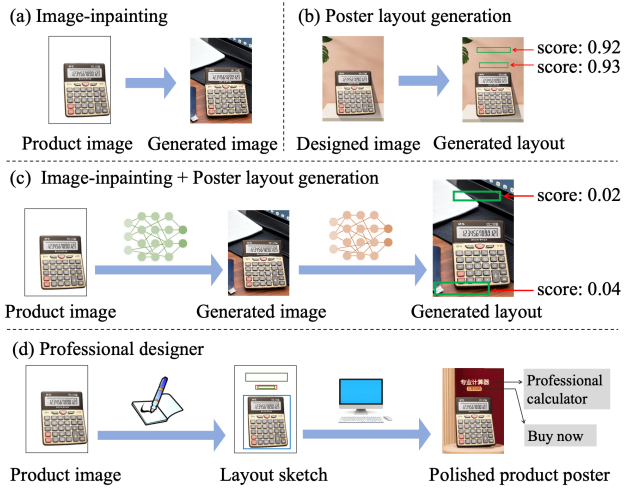


Figure 1. Two fields related to EPG: (a) Image-inpainting and (b) Poster layout generation. (c) The combination of (a) and (b) can be regarded as a naive solution to EPG. (d) The workflow of professional designers. “score” refers to the confidence of layout prediction, and the gray blocks are translations of texts. Green and red boxes represent texts and underlays, respectively.

visual components, such as underlays, texts, and the product but also have a pleasant background. This challenging task is typically undertaken by professional designers, which leads to low efficiency and high cost in poster production. To generate high-quality posters with low cost, we propose a new task, End-to-end product Poster Generation (EPG), which aims to generate an image that transmits the product messages to social groups given the product image and texts.

The most related fields to EPG are image-inpainting [1, 20, 26, 30, 31, 40, 41] and poster layout generation [13, 21, 36, 44]. As Figure 1 (a) and (b) show, the image-inpainting model completes the background of the poster based on the product image, and the poster layout generator plans the layout of visual components given a manually designed image. As Figure 1 (c) shows, simply combin-

ing the two methods can be regarded as a naive solution to EPG, where the result of the image-inpainting model can be put into the layout generator to arrange the visual components. However, this solution still has the following issues: 1) The background generated from the image-inpainting model may be too complex to display any text, which leads to a higher failure rate of layout prediction. 2) The image-inpainting methods pre-fix the location of the product, so that the layout generator can only arrange the locations of texts and underlays. This limits the diversity of poster design.

Let’s revisit how professional designers tackle the challenges of this task. As Figure 1 (d) shows, most designers use a hybrid process that consists of two stages [35]: Planning and rendering. At the planning stage, they sketch layouts of the product and other visual components to execute their ideas. The positions of other visual components get rid of the constraint of the predetermined product location, which contributes to the diversity of the layouts. At the rendering stage, they place the visual components based on the layout results and polish them on a computer. They consider the positions of texts when drawing the background, thereby avoiding that the drawn background is too complex to place texts.

Referring to the designing process of professional designers, we put forward the first product poster generation framework P&R shown as Figure 2. At the planning stage, we propose the PlanNet to generate layouts of products and other visual components. PlanNet firstly encodes the product image and the texts, and then fuses them with a layout decoder to predict more reasonable and flexible layouts. At the rendering stage, we propose the RenderNet to integrate layouts and the product image into control conditions, where a spatial fusion module is used to explore the spatial relationships among layouts generated by PlanNet, and the appearance of the product is also encoded to ensure harmony between the generated background and the product. Finally, these two control conditions are input to ControlNet [41], which can guide Stable Diffusion [31] to generate product posters with pleasant backgrounds and easy to convey information.

To train and evaluate our method, we construct the first product poster generation dataset PPG30k including appealing product posters, layouts of visual components, product masks, and text contents. We conduct comprehensive experiments on PPG30k, and the results indicate that our method performs better in terms of the rationality of the layout and the aesthetics of the image. The contributions of our paper are four-fold:

- We propose a new task EPG and the first product poster generation framework P&R, which can generate appealing posters to transmit product messages effectively.
- We put forward the PlanNet to plan the overall poster lay-

out, taking into account the product appearance and text content comprehensively.

- We put forward the RenderNet to render the overall layout into a poster image, where product images and layouts of visual components are integrated into multiple conditions to control the generation process.
- We build the first large-scale dataset PPG30k for training and evaluating the models of EPG.

2. Related Work

2.1. Layout Generation

Previous layout generation methods [2, 27, 28] mainly rely on heuristic algorithms and templates, which have limitations in the scope of application and lack diversity. With the advances in deep learning, a variety of deep models including GAN [8, 22, 36, 43, 44], VAE [17], transformers [3, 10, 15, 19, 33, 34, 39] and diffusion models [4, 12, 14, 16, 21], have been employed to learn the underlying patterns and structures of layouts from large datasets. These methods can be roughly classified into two types: content-agnostic and content-aware methods. Content-agnostic methods place elements on a blank canvas and thus have fewer constraints. Instead of directly synthesizing pixel-wise layout, LayoutGAN [22] predicted the labels and geometric parameters of elements. BLT [19] introduced a bidirectional transformer to generate all results simultaneously for faster speed and better controllability. LayoutDM [16] devised a diffusion framework for categorical variables in discrete space.

However, unaware of the visual contents, content-agnostic methods fail to yield satisfactory poster layouts. Therefore, content-aware methods that predict layouts based on pre-generated images are receiving increasing attention in poster layout generation tasks. CGL-GAN [44] and its subsequent work PDA-GAN [36] made attempts to narrow the domain gap between inpainted training images and clean testing images. DS-GAN [13] devised a CNN-LSTM framework to strike a balance between graphic and content-aware metrics. RADM [21] first introduced the diffusion model in poster layout generation. It gradually converts a set of random boxes to a plausible layout. Although these methods produce reasonable poster layouts, they have strict requirements for image content. When image composition is complex, they are unable to find suitable places for elements. Unlike existing methods, our proposed PlanNet enables planning of the overall layout, allowing the RenderNet to reserve places for visual elements.

2.2. Conditional Image Generation

The conditional generation models aim to generate images according to the given conditions. At the rendering stage of our poster generating system, the genera-

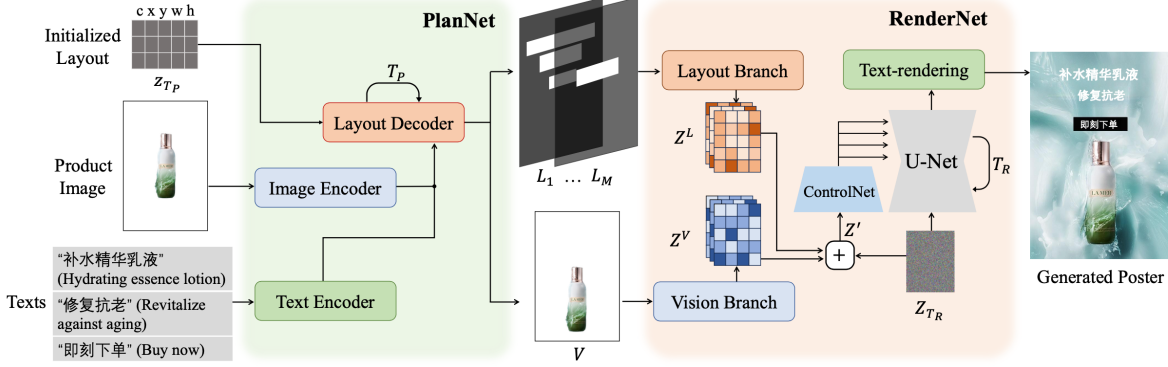


Figure 2. The framework of P&R. It consists of a PlanNet and a RenderNet. The PlanNet aims to generate layouts based on the product image and texts, and the RenderNet aims to generate posters based on the product image and the generated layouts from PlanNet. The gray blocks contain texts and translations in the brackets.

tor should consider the product image and the layout of visual components, which is related to the research of image-inpainting [1, 20, 26, 30, 31, 40, 41], and layout-to-image [5, 6, 11, 37, 38, 41, 42].

Image-inpainting methods complete the masked area of an image based on the known area. LaMa [30] proposed a Fast Fourier Convolution module to fill the image with higher receptive fields. Yu *et al.* [40] proposed a contextual attention layer to extract features from remote regions. With the rise of the diffusion model, more and more researchers proposed image-inpainting methods based on the Denoising Diffusion Probabilistic Models [1, 26, 31, 41]. For example, Stable Diffusion (SD) [31] used the U-Net [32] module to predict the noise with the given mask and image. ControlNet [41] regard the incomplete image as the condition and used an extra branch to control the inpainting process. To generate the background of product poster, the masked area is set as the background of the poster and should be completed based on the known area of the product. For example, Ku *et al.* [20] proposed a GAN-based method to produce the background of the product ads. They copied the background from the ads of a similar product and modified the image by the GAN-based inpainting method. Although these methods can generate realistic backgrounds, they may not be suitable for placing text due to the complexity of the patterns.

To strictly control the relative positions of the items in the images, many researches add the layout information as a restriction to generate images. Yang *et al.* [38] divided each layout image into several patches and fused the different layout images according to the position of the patch. Xue *et al.* [37] proposed a cross-attention module that aligned the text description with layout information, which can generate objects according to the text at the corresponding position. Zhang *et al.* [41] controlled the generation pro-

cess by incorporating layout image features into the original stable diffusion model. They introduced an additional encoder branch to introduce the extra control conditions to the pre-trained SD module. However, these methods generate the background without perceiving the product information, which leads to a mismatch between the style of the generated background and the product. Therefore, we integrate the product image into the layout-to-image generator, combining the advantages of image-inpainting and layout-to-image methods.

3. Method

The framework of P&R is shown as Figure 2, which consists of a PlanNet and a RenderNet. The PlanNet predicts the overall layout of the poster based on the given product image and texts, and then the RenderNet renders the predicted layout as a poster image. For the PlanNet, it first encodes the product image and texts with the image and text encoders. Then we input the encoded features to a layout decoder to learn the relationship among layout elements, image features, and text features. After a T_P -step denoising process, the initialized layout is restored to the overall layout of the poster. For the RenderNet, it utilizes the layout results generated by PlanNet with two branches. The first layout branch fuses the layouts of visual components into a unified layout embedding with a spatial fusion module, which can learn the spatial relationship among the different visual components. The second vision branch uses a series of convolution layers to extract the visual embeddings of the repositioned product, which contributes to generating a harmonious background with the product. Then extracted layout and visual embeddings are put into the ControlNet to guide the generation process of stable diffusion. After generating an image prepared for rendering texts, we use a text-rendering module to obtain the final product poster.

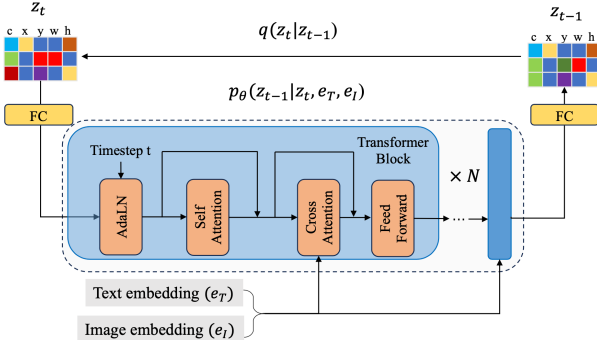


Figure 3. The architecture of the layout decoder.

3.1. PlanNet

A priori overall planning layout is beneficial for the downstream generation tasks. Although content-agnostic methods can predict the overall layout, they neglect the appearance of the product and the text content, making it difficult to achieve a good visual balance. To address this issue, we propose the PlanNet, which considers the product and text information simultaneously while predicting the overall layout. The layout consists of a set of elements, which are represented by five attributes c, x, y, w, h , where c is the category, (x, y) is the center point, and w, h are the width and height. Each attribute has K different values. To handle discrete variables, the PlanNet is based on discrete diffusion models including diffusion and denoising processes.

In the diffusion process, we denote attribute at time t as $z_t, z_t \in \{1, 2, \dots, K\}$. The probability of transition from z_{t-1} to z_t is defined as $[Q_t]_{ij} = q(z_t = i | z_{t-1} = j)$, and the state transition matrix \mathbf{Q}_t is defined as the following:

$$\mathbf{Q}_t = \begin{bmatrix} \alpha_t & \beta_t & \beta_t & \dots & 0 \\ \beta_t & \alpha_t & \beta_t & \dots & 0 \\ \beta_t & \beta_t & \alpha_t & \dots & 0 \\ \vdots & \vdots & \vdots & \ddots & \vdots \\ \gamma_t & \gamma_t & \gamma_t & \gamma_t & 1 \end{bmatrix}, \quad (1)$$

where $\alpha_t, \beta_t, \gamma_t$ are the probabilities to keep the same state, change to other states, and change to [MASK] state [9] at timestep t , respectively. Once the attribute changes to [MASK] state, it will not change to other states. When t is sufficiently large, all states will eventually fall into [MASK] state. The forward process in matrix format can be written as:

$$q(z_t | z_{t-1}) = \mathbf{v}^T(z_t) \mathbf{Q}_t \mathbf{v}(z_{t-1}), \quad (2)$$

where $\mathbf{v}(z_t)$ is a column one-hot vector of z_t . Due to the property of Markov chain $q(z_t | z_{t-1}, z_0) = q(z_t | z_{t-1})$, the probability of transition from z_0 to z_t can be simplified as:

$$q(z_t | z_0) = \mathbf{v}^T(z_t) \mathbf{Q}_t \mathbf{Q}_{t-1} \dots \mathbf{Q}_1 \mathbf{v}(z_0). \quad (3)$$

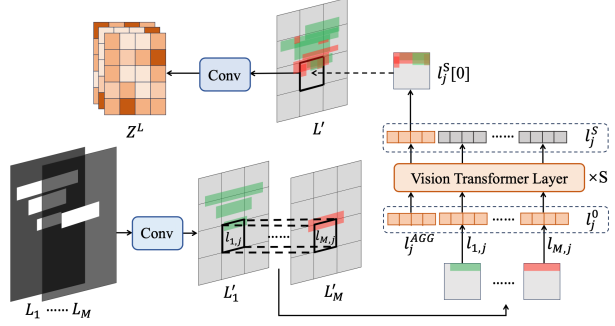


Figure 4. The architecture of the spatial fusion module.

Conditioned on z_0 , we can also calculate the posterior of diffusion process by:

$$q(z_{t-1} | z_t, z_0) = \frac{q(z_t | z_{t-1}, z_0) q(z_{t-1} | z_0)}{q(z_t | z_0)}. \quad (4)$$

In the denoising process, we use the trained PlanNet to convert initialized layout z_{T_P} to z_0 . PlanNet consists of an image encoder, a text encoder, and a layout decoder. To make the encoders better adapted to e-commerce scenarios, we have collected over 30 million image-text pairs from the e-commerce platform, and finetune ALBEF [23] following its original training objectives, including image-text contrastive learning, masked language model, and image-text matching. Besides, we add another training objective which aims to predict the category of product based on image and texts. Following the configuration in ALBEF, the image encoder is a 12-layer visual transformer ViT-B/16 [7], and the text encoder is the first 6 layers of RoBERTa [24] pretrained with Chinese. However, it is worth noting that our method is not limited to Chinese. By changing the pre-trained text encoder, other languages can also be supported.

Then the layout decoder uses the extracted text and image embeddings to estimate the reverse process from z_t to z_{t-1} . As shown in Figure 3, it is comprised of two fully connected (FC) layers and N transformer blocks. Firstly, z_t is projected to element embedding e_t^0 with an FC layer. After N transformer blocks, the element embedding e_t^{N-1} is decoded into z_{t-1} with another FC layer. In each transformer block, the time step t is combined with element embedding e_t using an adaptive layer normalization (AdaLN) and a self-attention (SA) layer:

$$h_t = \text{AdaLN}(e_t, t), \quad (5)$$

$$a_t = h_t + \text{SA}(h_t). \quad (6)$$

Then the cross-attention (CA) is calculated using the result of self attention and the concatenation of text embedding e_T and image embeddings e_I :

$$e_t = \text{FF}(a_t + \text{CA}(a_t, \text{CAT}(e_T, e_I))), \quad (7)$$

where CAT is concatenation and FF is the feed forward function.

3.2. RenderNet

The background generated by image-inpainting methods may fail to place texts because of the complex patterns, therefore we put forward the RenderNet that incorporates layout information generated by PlanNet into the image-inpainting. RenderNet consists of a layout branch, a vision branch, Stable Diffusion (SD) [31], ControlNet [41] and a text-rendering module. The layout branch aims to encode layouts of visual components. To better represent the spatial information of layouts, we transform the coordinate information from the PlanNet to masked layout images $\{L_m\}$, where $m = 1, \dots, M$ and M is the category number of visual components. For L_m , the areas of the m -th type of visual component are filled with 1 and the rest area is 0. To exploit the spatial relationship among M layouts, we put forward a spatial fusion module shown as Figure 4.

Firstly, we use a three-layer convolution network to encode $\{L_m\}$ to latent representations $\{L'_m\}$, where $L'_m \in \mathbb{R}^{C \times W \times H}$. Then we fuse $\{L'_m\}$ into a unified layout representation L' . Specifically, L'_m are divided into patches $\{l_{m,j}\}$ with the shape of $C \times P \times P$, where j is the index of the patch and $j = 1, \dots, W/P * H/P$. To obtain the j -th patch of L' , we fuse the j -th patch of different L'_m as follows:

$$l_j^0 = \text{CAT}(l_j^{\text{AGG}}, l_{1,j}, \dots, l_{M,j}), \quad (8)$$

where CAT is concatenation and l_j^{AGG} is an aggregation token added to the input. Then l_j^0 is input into a S -layer vision transformer:

$$l_j^s = \text{MHSA}(l_j^{s-1}) + l_j^{s-1}, \quad (9)$$

$$l_j^s = \text{FF}(l_j^s) + l_j^s, \quad (10)$$

where MHSA(\cdot) is the multi-head self-attention function, and FF(\cdot) is a linear network with layer normalization. We use the $l_j^S[0]$ as the j -th patch of L' . Finally, we apply a three-layer convolution network on L' to get the layout embedding Z^L .

The vision branch aims to perceive the visual and spatial information of the product. We firstly zoom and move the product image based on the coordinate information from PlanNet to get a repositioned product image V . Then we apply a six-layer convolution network on V to extract the visual embedding Z^V . Finally, the visual and layout embeddings are added into ControlNet $\epsilon_\theta^c(\cdot)$ as control condition to guide SD.

At the training stage, we encode the prompt as τ by a text encoder τ_θ of the pre-trained CLIP [29]. At the t -th time-step, a random noise ϵ is added to the embedding of the training image Z to produce the noised feature Z_t . Then,



Figure 5. Some visual examples in PPG30k.

we use a U-Net $\epsilon_\theta(\cdot)$ to predict the added noise ϵ . The loss function can be formulated as follows:

$$\mathcal{L} = \mathbb{E}_{Z, \tau, t, \epsilon \sim \mathcal{N}(0, 1)} [\|\epsilon - \epsilon_\theta(Z_t, t, \tau_\theta(\tau), \epsilon_\theta^c(Z'))\|_2^2], \quad (11)$$

where $Z' = Z_t + Z^L + Z^V$.

At the inference stage, the well-trained RenderNet predicts the noise added to an image for T_R steps, given a random noise Z_{T_R} , text embedding τ , the control condition $\epsilon_\theta^c(Z')$. After removing the noise, we obtain the image prepared for placing texts.

As it is insufficient to train a visual text generation model solely on the poster image dataset, we introduce an extra text-rendering module to render texts on the generated image heuristically. We choose the appropriate text color based on the main color of the text area, and then randomly select fonts from the font library. The code will be released and we will focus on integrating a visual text generation model into the RenderNet in the future.

4. Dataset

To promote research in this field, we construct the first large-scale end-to-end product poster generation dataset PPG30k. The images are collected from CGL-Dataset [44], where we remove posters with portraits to avoid portrait rights disputes, and posters with unsightly backgrounds to improve generation quality. The selected images are with pleasing backgrounds and can effectively transmit messages, as shown in Figure 5. Eventually, there are 32724 training images and 1426 testing images in PPG30k, and the image size is 513×750 .

As illustrated in Figure 6 (a), there are three types of elements including texts, underlays, and products. The geometric attributes $\{x, y, w, h\}$ and categories c are annotated. Besides, as texts play an important role in conveying messages in posters, the corresponding textual contents are also

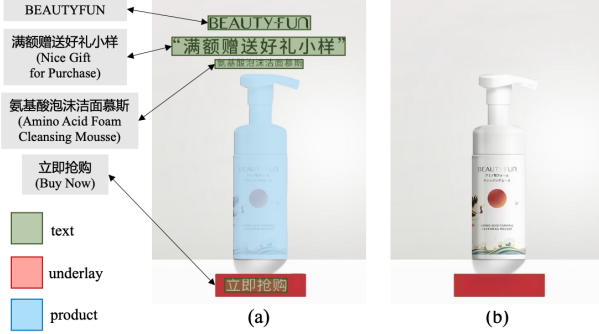


Figure 6. (a) Poster layout annotations. Product, texts and underlays are annotated. The texts in gray boxes are the translations of the texts on the posters (b) The clean image. The texts on the poster are erased while underlays are retained.

recorded. To get the precise product appearance, products are annotated with masks. When training the PlanNet, we use the smallest rectangular area that can surround the product as its location. The PlanNet takes the textual contents and product images as input, and the location and categories are the ground truth. For convenience, we will release extracted image and text embeddings. When training the RenderNet, we convert the location of texts and underlays to masks. As shown in Figure 6 (b), the RenderNet takes the masks and product images as input, and the clean images are used as ground truth where texts are erased.

5. Experiments

5.1. Implementation Details

For the PlanNet, there are 4 transformer blocks with 8 attention heads, 512 embedding dimensions, and 2048 hidden dimensions, and we set the dropout rate 0.1. The diffusion timesteps T_P is 100. We train the PlanNet for 100 epochs using AdamW optimizer [25] with a learning rate of 5.0×10^{-4} . For the RenderNet, we train it for 500 epochs with the same optimizer as ControlNet [41]. The prompt is uniformly set as “a poster of an e-commerce product”. We resize the image to 256×384 . The hidden feature map of the spatial fusion module satisfies $C = 320, W = 128, H = 192$. The layer number S is 2, the inference step T_R is 50, and the patch size P is 8.

5.2. Evaluation Metrics

Numerical Metrics. To evaluate the PlanNet, Frechet Inception Distance for layout (FID-layout) [16] is used to measure the similarity between the generated and ground truth layouts. Maximum Intersection over Union (Max IoU) [18] is used to compute the average IoU between the optimal matching between the generated boxes and the ground truth with the same category. To evaluate the Ren-

Method	FID-image ↓	CLIP-score ↑	BQ ↑	LR ↑
SD-ipt [31]	47.30	87.60	2.20	2.06
CN-ipt [41]	67.19	79.54	1.34	1.79
LaMa [30]	50.59	87.89	2.82	2.88
P&R	35.23	91.80	3.66	3.24

Table 1. Comparison results with SOTA poster generators, which consist of the image-inpainting method and CGL-GAN [44]. “SD-ipt” and “CN-ipt” refer to the inpainting version of stable diffusion and ControlNet.

derNet, Frechet Inception Distance for image (FID-image) is used to measure the distance between the distributions of generated and real images. CLIP-score [29] is used to calculate the cosine similarity between the features of generated and real images, which are extracted by the image encoder of a pre-trained CLIP model.

User Study. To evaluate the quality of the poster, we conduct a user study on 20 experienced advertising practitioners. In this study, we use 100 groups of images, where each group contains 4 posters generated by different methods. All these results in each group are presented side-by-side and in a random order. Practitioners are asked to rank them from the perspectives of background quality (BQ) and layout rationality (LR), where 1 is the worst and 4 is the best. When ranking the BQ, the practitioners focus on the suitability of serving as the product poster and the harmony between the background and the product. When ranking the LR, the practitioners consider the overlap of different components and the visual balance of components on the poster. To evaluate the performances of poster layout generators, we use 100 groups of layouts, where each group contains 4 randomly ordered layouts generated by different methods. Practitioners are asked to judge whether the layout result is qualified (R_{pass}) and select the best layout (R_{best}). When evaluating the two metrics, practitioners consider the overlap of different components and, rationality of visual components.

5.3. Quantitative Analysis

Comparison with SOTA Poster Generators. As mentioned above, combining image-inpainting and poster layout generation methods can be seen as a naive solution to EPG. To verify the superiority of P&R, we combine three image-inpainting methods with a SOTA layout generator CGL-GAN [44] and compare their generated posters with ours.

As Table 1 shows, our method performs the best on FID-image and CLIP-score, which indicates that the style of background images generated by our RenderNet is closer to that of product posters. We also calculate the average BQ and LR. The results show that the images generated by our

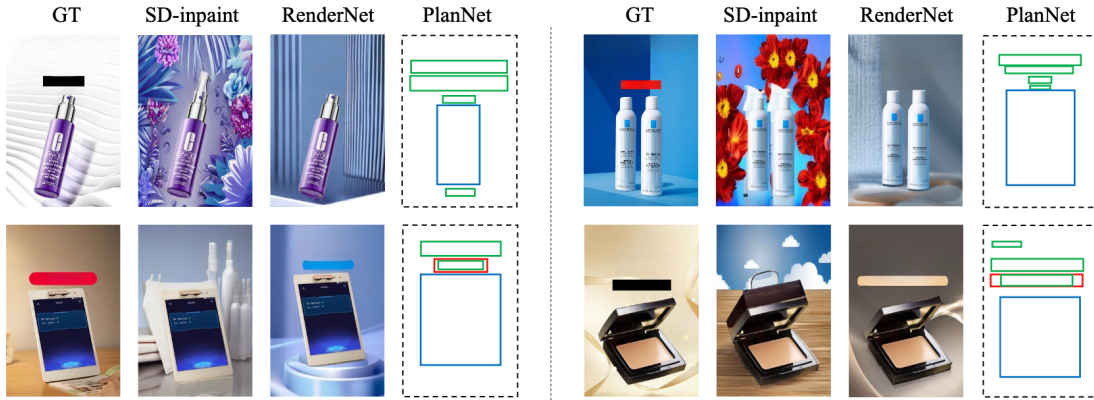


Figure 7. Qualitative comparison with SD-inpaint. “GT” refers to the ground truth. The green, red and blue boxes respectively represent texts, underlays and the product (the same below).

Method	FID-layout ↓	Max IoU ↑	FID-image ↓	CLIP-score ↑	R _{pass} ↑	R _{best} ↑
LayoutDM [16]	15.60	0.51	38.97	89.89	53.95%	20.65%
FlexDM [15]	107.33	0.21	52.88	81.20	58.40%	24.60%
BoxNet [34]	93.54	0.35	43.60	88.28	39.85%	12.35%
P&R	14.50	0.58	35.23	91.80	70.85%	42.40%

Table 2. Comparison results with SOTA layout generators.

Method	FID-image ↓	CLIP-score ↑
CN-lyt [41]	44.31	69.92
Freestyle [37]	68.68	60.11
P&R	33.55	91.46

Table 3. Comparison results with SOTA conditional image generators. “CN-lyt” refers to the layout-to-image version of ControlNet.

Text	Image	FID-layout ↓	Max IoU ↑
✓	✓	14.50	0.58
✓		17.15	0.55
	✓	18.42	0.52
		21.05	0.51

Table 4. Ablation study of image and text contents.

method are more suitable to serve as product posters, and our generated layouts achieve a better visual balance.

We take the SD-inpaint method as an example to compare our method with SOTA poster generators qualitatively. As Figure 7 shows, although the SD-inpaint method can generate realistic background images, the content of the background images is too complex to have sufficient space for visual components, which results in a high failure rate of layout generation. Our method can generate an appeal-

ing background with the superiority of transmitting product information.

Comparison with SOTA Layout Generators. To verify the advantages of our PlanNet, we compare the PlanNet with SOTA layout generators, including LayoutDM [16], FlexDM [15] and BoxNet [34]. Based on their official codes, we train these models on PPG30k. The comparison result is shown in Table 2. Because of making fuller use of text and image features, our method achieves the best on FID-layout and Max IoU metrics. Additionally, to verify the impact of layout on background generation, we use the RenderNet to generate background based on the layout results of four methods. The images generated from the results of the PlanNet achieve the best on FID-image and CLIP-score metrics, which proves that our PlanNet is more beneficial for downstream image generation. Meanwhile, the result of the user study indicates that our PlanNet arranges various elements with better composition.

Comparison with SOTA Conditional Generators. Layout-to-image methods ignore the product content when generating posters, resulting in the generated background may not match the style of the product. Our RenderNet combines the advantages of both image-inpainting and layout-to-image methods, which can give attention to both layouts and the product. To verify this, we compare two state-of-the-art layout-to-image methods based on the ground truth layouts. Table 3 indicates that back-

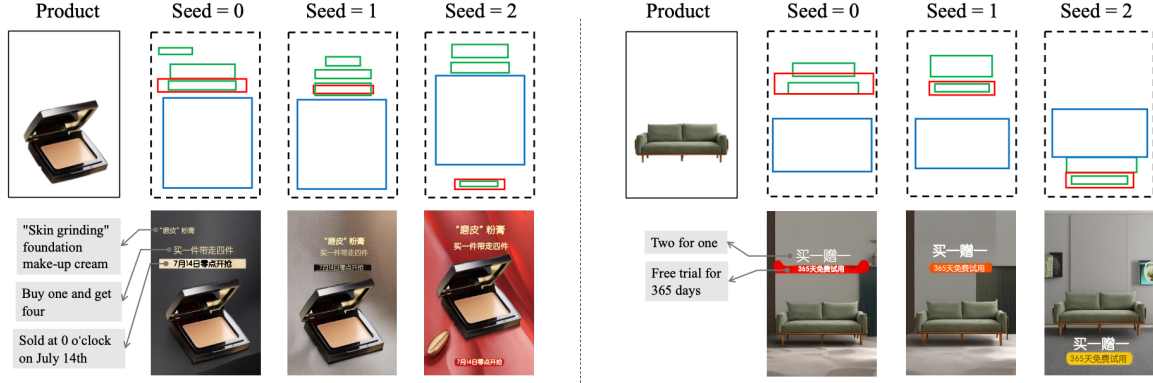


Figure 8. Generated posters under different random seeds. The texts in gray boxes are the translations of the texts on the posters.

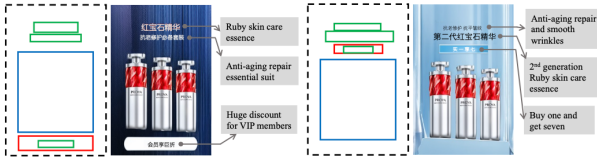


Figure 9. Generated results under different text contents. The texts in gray boxes are the translations of the texts on the posters.

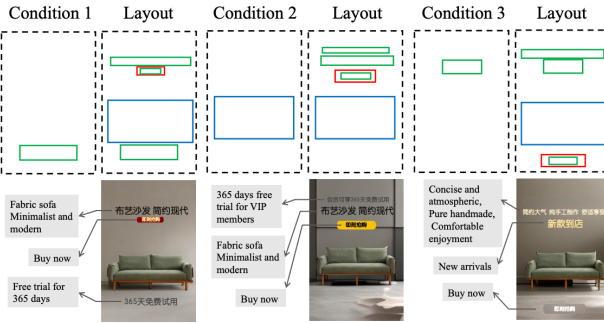


Figure 10. Generated results under different layout conditions. The texts in gray boxes are the translations of the texts on the posters.

grounds generated by our method match the product more harmoniously.

Effects of Image and Text Contents. To verify the influence of image and text contents on the layout, we remove the image encoder, text encoder, and both of them to train three variants of the PlanNet on PPG30k. As Table 4 shows, removing image, text contents results in 2.65, 3.92 reduction on FID-layout and 0.03, 0.06 reduction on Max IoU, respectively. Removing both results in further performance degradation, which proves the significance of considering image and text contents in poster layout generation.

5.4. Qualitative Analysis

Diversity. To show the diversity of P&R, we set different random seeds to generate posters. As shown in Figure 8, the leftmost column is the input product and texts. In the rest part, the first row is the different layouts and the second row is the posters generated based on the layouts above. This shows that our method can generate a variety of reasonable layouts and appealing posters.

Different Text Contents. To verify that our method can effectively understand text contents, we keep the random seed unchanged and use different text contents as input. The result is shown in Figure 9, which proves that our method can produce appropriate layouts and posters based on different text contents.

Partial Layout Condition. Since our method supports that pre-defined conditions can be injected into the element embedding, users can pre-set the position, size, and category of the elements according to their own preferences. In Figure 10, we show the results under three commonly used layout conditions. From left to right, we set a text at the bottom, a product in the middle, and a text at the top, respectively. The generated results show that our method performs well in completing the entire layouts and posters based on partial layout conditions.

6. Conclusion

We propose a novel product poster generation framework named P&R, which can generate product posters with well-designed layouts and visually appealing backgrounds. In P&R, a PlanNet is firstly used to plan the overall layout, which merges the product image and text contents. This facilitates the creation of a well-organized layout. Then a RenderNet employs a spatial fusion module to incorporate the layouts generated by PlanNet, and encodes the appearance of the product to ensure a harmonious blend between the generated background and the product image. To pro-

mote research in this field, we construct the PPG30k dataset for end-to-end product poster generation task. Extensive experiments on PPG30k demonstrate that P&R surpasses state-of-the-art methods in terms of layout prediction and poster quality. In the future, we will focus on integrating the visual text generation model into a unified framework.

References

- [1] Omri Avrahami, Dani Lischinski, and Ohad Fried. Blended diffusion for text-driven editing of natural images. In *Proceedings of the IEEE/CVF Conference on Computer Vision and Pattern Recognition*, pages 18208–18218, 2022. 1, 3
- [2] Ying Cao, Antoni B Chan, and Rynson WH Lau. Automatic stylistic manga layout. *ACM Transactions on Graphics*, 31(6):1–10, 2012. 2
- [3] Yunning Cao, Ye Ma, Min Zhou, Chuanbin Liu, Hongtao Xie, Tiezheng Ge, and Yuning Jiang. Geometry aligned variational transformer for image-conditioned layout generation. In *Proceedings of the 30th ACM International Conference on Multimedia*, 2022. 2
- [4] Shang Chai, Liansheng Zhuang, and Fengying Yan. Layoutdm: Transformer-based diffusion model for layout generation. In *Proceedings of the IEEE/CVF Conference on Computer Vision and Pattern Recognition*, pages 18349–18358, 2023. 2
- [5] Minghao Chen, Iro Laina, and Andrea Vedaldi. Training-free layout control with cross-attention guidance. *arXiv preprint arXiv:2304.03373*, 2023. 3
- [6] Guillaume Couairon, Marlène Careil, Matthieu Cord, Stéphane Lathuilière, and Jakob Verbeek. Zero-shot spatial layout conditioning for text-to-image diffusion models. In *Proceedings of the IEEE/CVF International Conference on Computer Vision*, pages 2174–2183, 2023. 3
- [7] Alexey Dosovitskiy, Lucas Beyer, Alexander Kolesnikov, Dirk Weissenborn, Xiaohua Zhai, Thomas Unterthiner, Mostafa Dehghani, Matthias Minderer, Georg Heigold, Sylvain Gelly, et al. An image is worth 16x16 words: Transformers for image recognition at scale. *arXiv preprint arXiv:2010.11929*, 2020. 4
- [8] Ian Goodfellow, Jean Pouget-Abadie, Mehdi Mirza, Bing Xu, David Warde-Farley, Sherjil Ozair, Aaron Courville, and Yoshua Bengio. Generative adversarial nets. *Advances in neural information processing systems*, 27, 2014. 2
- [9] Shuyang Gu, Dong Chen, Jianmin Bao, Fang Wen, Bo Zhang, Dongdong Chen, Lu Yuan, and Baining Guo. Vector quantized diffusion model for text-to-image synthesis. In *Proceedings of the IEEE/CVF Conference on Computer Vision and Pattern Recognition*, pages 10696–10706, 2022. 4
- [10] Kamal Gupta, Justin Lazarow, Alessandro Achille, Larry S. Davis, Vijay Mahadevan, and Abhinav Shrivastava. Layout-transformer: Layout generation and completion with self-attention. In *Proceedings of the IEEE/CVF International Conference on Computer Vision*, pages 1004–1014, 2021. 2
- [11] Sen He, Wentong Liao, Michael Ying Yang, Yongxin Yang, Yi-Zhe Song, Bodo Rosenhahn, and Tao Xiang. Context-aware layout to image generation with enhanced object appearance. In *Proceedings of the IEEE/CVF Conference on Computer Vision and Pattern Recognition*, pages 15049–15058, 2021. 3
- [12] Jonathan Ho, Ajay Jain, and Pieter Abbeel. Denoising diffusion probabilistic models. *Advances in neural information processing systems*, 33:6840–6851, 2020. 2
- [13] Hsiao Yuan Hsu, Xiangteng He, Yuxin Peng, Hao Kong, and Qing Zhang. Posterlayout: A new benchmark and approach for content-aware visual-textual presentation layout. In *Proceedings of the IEEE/CVF Conference on Computer Vision and Pattern Recognition*, pages 6018–6026, 2023. 1, 2
- [14] Mude Hui, Zhizheng Zhang, Xiaoyi Zhang, Wenxuan Xie, Yuwang Wang, and Yan Lu. Unifying layout generation with a decoupled diffusion model. In *Proceedings of the IEEE/CVF Conference on Computer Vision and Pattern Recognition*, pages 1942–1951, 2023. 2
- [15] Naoto Inoue, Kotaro Kikuchi, Edgar Simo-Serra, Mayu Otani, and Kota Yamaguchi. Towards Flexible Multi-modal Document Models. In *Proceedings of the IEEE/CVF Conference on Computer Vision and Pattern Recognition*, pages 14287–14296, 2023. 2, 7
- [16] Naoto Inoue, Kotaro Kikuchi, Edgar Simo-Serra, Mayu Otani, and Kota Yamaguchi. LayoutDM: Discrete Diffusion Model for Controllable Layout Generation. In *Proceedings of the IEEE/CVF Conference on Computer Vision and Pattern Recognition*, pages 10167–10176, 2023. 2, 6, 7
- [17] Akash Abdu Jyothi, Thibaut Durand, Jiawei He, Leonid Sigal, and Greg Mori. Layoutvae: Stochastic scene layout generation from a label set. In *Proceedings of the IEEE/CVF International Conference on Computer Vision*, pages 9895–9904, 2019. 2
- [18] Kotaro Kikuchi, Edgar Simo-Serra, Mayu Otani, and Kota Yamaguchi. Constrained graphic layout generation via latent optimization. In *Proceedings of the 29th ACM International Conference on Multimedia*, pages 88–96, 2021. 6
- [19] Xiang Kong, Lu Jiang, Huiwen Chang, Han Zhang, Yuan Hao, Haifeng Gong, and Irfan Essa. Blt: bidirectional layout transformer for controllable layout generation. In *European Conference on Computer Vision*, pages 474–490. Springer, 2022. 2
- [20] Yueh-Ning Ku, Mikhail Kuznetsov, Shaunak Mishra, and Paloma de Juan. Staging e-commerce products for online advertising using retrieval assisted image generation. *arXiv preprint arXiv:2307.15326*, 2023. 1, 3
- [21] Fengheng Li, An Liu, Wei Feng, Honghe Zhu, Yaoyu Li, Zheng Zhang, Jingjing Lv, Xin Zhu, Junjie Shen, Zhangang Lin, and Jingping Shao. Relation-aware diffusion model for controllable poster layout generation. In *Proceedings of the 32nd ACM International Conference on Information and Knowledge Management*, page 1249–1258, 2023. 1, 2
- [22] Jianan Li, Jimei Yang, Aaron Hertzmann, Jianming Zhang, and Tingfa Xu. Layoutgan: Generating graphic layouts with wireframe discriminators. In *International Conference on Learning Representations*, 2019. 2
- [23] Junnan Li, Ramprasaath Selvaraju, Akhilesh Gotmare, Shafiq Joty, Caiming Xiong, and Steven Chu Hong Hoi. Align before fuse: Vision and language representation learning with momentum distillation. *Advances in neural information processing systems*, 34:9694–9705, 2021. 4

- [24] Yinhan Liu, Myle Ott, Naman Goyal, Jingfei Du, Mandar Joshi, Danqi Chen, Omer Levy, Mike Lewis, Luke Zettlemoyer, and Veselin Stoyanov. Roberta: A robustly optimized bert pretraining approach. *ArXiv*, abs/1907.11692, 2019. 4
- [25] Ilya Loshchilov and Frank Hutter. Decoupled weight decay regularization. *arXiv preprint arXiv:1711.05101*, 2017. 6
- [26] Andreas Lugmayr, Martin Danelljan, Andres Romero, Fisher Yu, Radu Timofte, and Luc Van Gool. Repaint: Inpainting using denoising diffusion probabilistic models. In *Proceedings of the IEEE/CVF Conference on Computer Vision and Pattern Recognition*, pages 11461–11471, 2022. 1, 3
- [27] Peter O’Donovan, Aseem Agarwala, and Aaron Hertzmann. Learning layouts for single-pagegraphic designs. *IEEE Transactions on Visualization and Computer Graphics*, 20: 1200–1213, 2014. 2
- [28] X. Pang, Ying Cao, Rynson W. H. Lau, and Antoni B. Chan. Directing user attention via visual flow on web designs. *ACM Transactions on Graphics*, 35:1 – 11, 2016. 2
- [29] Alec Radford, Jong Wook Kim, Chris Hallacy, Aditya Ramesh, Gabriel Goh, Sandhini Agarwal, Girish Sastry, Amanda Askell, Pamela Mishkin, Jack Clark, et al. Learning transferable visual models from natural language supervision. In *International conference on machine learning*, pages 8748–8763, 2021. 5, 6
- [30] Suvorov Roman, Logacheva Elizaveta, Mashikhin Anton, Remizova Anastasia, Ashukha Arsenii, Silvestrov Aleksei, Kong Naejin, Goka Harshith, Park Kiwoong, and Lempitsky. Victor. Resolution-robust large mask inpainting with fourier convolutions. In *Proceedings of the IEEE/CVF winter conference on applications of computer vision*, page 2149–2159, 2022. 1, 3, 6
- [31] Robin Rombach, Andreas Blattmann, Dominik Lorenz, Patrick Esser, and Björn Ommer. High-resolution image synthesis with latent diffusion models. In *Proceedings of the IEEE/CVF Conference on Computer Vision and Pattern Recognition*, pages 10684–10695, 2022. 1, 2, 3, 5, 6
- [32] Olaf Ronneberger, Philipp Fischer, and Thomas Brox. U-net: Convolutional networks for biomedical image segmentation. In *Medical Image Computing and Computer-Assisted Intervention*, pages 234–241. Springer, 2015. 3
- [33] Ashish Vaswani, Noam Shazeer, Niki Parmar, Jakob Uszkoreit, Llion Jones, Aidan N Gomez, Łukasz Kaiser, and Illia Polosukhin. Attention is all you need. *Advances in neural information processing systems*, 30, 2017. 2
- [34] Ruichen Wang, Zekang Chen, Chen Chen, Jian Ma, Haonan Lu, and Xiaodong Lin. Compositional text-to-image synthesis with attention map control of diffusion models. *arXiv preprint arXiv:2305.13921*, 2023. 2, 7
- [35] Wikipedia. Graphic design. In https://en.wikipedia.org/wiki/Graphic_design. 2
- [36] Chenchen Xu, Min Zhou, Tiezheng Ge, Yuning Jiang, and Weiwei Xu. Unsupervised domain adaption with pixel-level discriminator for image-aware layout generation. In *Proceedings of the IEEE/CVF Conference on Computer Vision and Pattern Recognition*, pages 10114–10123, 2023. 1, 2
- [37] Han Xue, Zhiwu Huang, Qianru Sun, Li Song, and Wenjun Zhang. Freestyle layout-to-image synthesis. In *Proceedings of the IEEE/CVF Conference on Computer Vision and Pattern Recognition*, pages 14256–14266, 2023. 3, 7
- [38] Binbin Yang, Yi Luo, Ziliang Chen, Guangrun Wang, Xiaodan Liang, and Liang Lin. Law-diffusion: Complex scene generation by diffusion with layouts. In *Proceedings of the IEEE/CVF International Conference on Computer Vision*, pages 22669–22679, 2023. 3
- [39] Cheng-Fu Yang, Wan-Cyuan Fan, Fu-En Yang, and Yu-Chiang Frank Wang. Layouttransformer: Scene layout generation with conceptual and spatial diversity. In *Proceedings of the IEEE/CVF Conference on Computer Vision and Pattern Recognition*, pages 3732–3741, 2021. 2
- [40] Jiahui Yu, Zhe Lin, Jimei Yang, Xiaohui Shen, Xin Lu, and Thomas S Huang. Generative image inpainting with contextual attention. In *Proceedings of the IEEE conference on computer vision and pattern recognition*, pages 5505–5514, 2018. 1, 3
- [41] Lvmin Zhang, Anyi Rao, and Maneesh Agrawala. Adding conditional control to text-to-image diffusion models. In *Proceedings of the IEEE/CVF International Conference on Computer Vision*, pages 3836–3847, 2023. 1, 2, 3, 5, 6, 7
- [42] Guangcong Zheng, Xianpan Zhou, Xuewei Li, Zhongang Qi, Ying Shan, and Xi Li. Layoutdiffusion: Controllable diffusion model for layout-to-image generation. In *Proceedings of the IEEE/CVF Conference on Computer Vision and Pattern Recognition*, pages 22490–22499, 2023. 3
- [43] Xinru Zheng, Xiaotian Qiao, Ying Cao, and Rynson WH Lau. Content-aware generative modeling of graphic design layouts. *ACM Transactions on Graphics*, 38(4):1–15, 2019. 2
- [44] Min Zhou, Chenchen Xu, Ye Ma, Tiezheng Ge, Yuning Jiang, and Weiwei Xu. Composition-aware graphic layout gan for visual-textual presentation designs. In *Proceedings of the Thirty-First International Joint Conference on Artificial Intelligence*, pages 4995–5001, 2022. 1, 2, 5, 6